EUROPEAN COMMISSION
6th EURATOM FRAMEWORK PROGRAMME

Oxidation and Release of Ruthenium from White Inclusions

(Experimental Study)

N. Vér[1)], L. Matus[1)], M. Kunstár[1)], A. Pintér[1)], J. Osán[1)], Z. Hózer[1)], B. Tóth[2)]

1) Hungarian Academy of Sciences, KFKI Atomic Research Institute
2) European Commission, Joint Research Centre, Institute for Energy, The Netherlands

DG JRC
Institute for Energy

March 2007

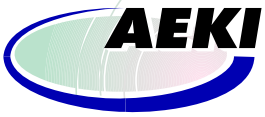

EUR 22730 EN

KFKI Atomic Energy Research Institute
Hungarian Academy of Sciences

Mission of the Institute for Energy
The Institute for Energy provides scientific and technical support for the conception, development, implementation and monitoring of community policies related to energy. Special emphasis is given to the security of energy supply and to sustainable and safe energy production.

European Commission
Directorate-General Joint Research Centre (DG JRC)
http://www.jrc.ec.europa.eu/

Institute for Energy, Petten (the Netherlands)
http://ie.jrc.ec.europa.eu/

Contact details:
B. Toth
Phone.: +31 (0) 224 56 5007
E-mail: bela.toth@jrc.nl

N. Ver
Phone: +36 (1) 392 2222
E-mail: nver@sunserv.kfki.hu

EUR 22730 EN
ISSN 1018-5593
Luxembourg: Office for Official Publications of the European Communities

EUROPEAN COMMISSION
6th EURATOM FRAMEWORK PROGRAMME

Oxidation and Release of Ruthenium from White Inclusions

(Experimental Study)

N. Vér[1)], L. Matus[1)], M. Kunstár[1)], A. Pintér[1)], J. Osán[1)], Z. Hózer[1)], B. Tóth[2)]

1) Hungarian Academy of Sciences, KFKI Atomic Research Institute
2) European Commission, Joint Research Centre, Institute for Energy, The Netherlands

March 2007

EUROPEAN COMMISSION
DIRECTORATE-GENERAL
Joint Research Centre
Institute for Energy

EUR 22730 EN

FP6 Action no. 3131
Contract No. 100997

AEKI-FRL-2006-409-01/01
KFKI Atomic Energy Research Institute
Hungarian Academy of Sciences

Executive Summary

In this paper the laboratory test results on oxidation and release of ruthenium as a fission product element are summarised. The ruthenium appears in the nuclear fuel pellets of pressurized water reactors as one of the fission product elements during burnup. In case of severe accident when the air can contact the degraded hot fuel, the ruthenium oxidises and its gaseous oxides, especially the RuO_4, release rapidly from the pellets to the environment. Because of high radio- and chemotoxicity of ruthenium tetra-oxide further experimental study of oxidation and release is essential.

It is well known that ruthenium in the irradiated fuel UO_2 fuel appears in small metallic alloy precipitations together with fission product elements such as Mo, Rh, Pd and Tc. The precipitations are seen in the metallographic pictures as white inclusions. This separate effect study focused on the differences in the release rate of gaseous ruthenium oxides when pure ruthenium or Mo-Ru-Rh-Pd metallic alloy is present in the simulated nuclear fuel. The oxidation and release were studied at constant reaction temperatures of 1000 ºC or 1100 ^{o}C.

The tests showed that during high-temperature oxidation of the Mo-Ru-Rh-Pd alloy in air flow the release rate of gaseous ruthenium oxides is reduced to 60-80% compared to the value measured in case of oxidation of pure metallic ruthenium powder in the same thermal-hydraulic conditions. Furthermore, if additional elements and chemical compounds representing other fission products were added in the alloy, a time delay of 30 to 60 minutes appeared in the release of gaseous ruthenium to the room-temperature environment similarly to earlier experiments conducted with the mixture of ruthenium powder and fission products.

One of the main results was that in the outlet air flow reaching the environment the partial pressure of RuO_4 was far above what could be expected for room-temperature equilibrium conditions. It was pointed out that the highly volatile RuO_4 can decompose in solid, non-volatile RuO_2 and O_2. The X-ray fluorescence analysis results showed that some ruthenium compounds deposited on the colder circuit walls of the test facility. This suggests RuO_4 is not fully airstable, i.e., its stability in air can be limited in time.

Contents

List of tables

List of figures

1. Introduction

In the previous years our laboratory performed the series of RUSET experiments to study the release of gaseous ruthenium from simulated spent fuel elements in severe accident conditions accompanied by air ingress [1-3]. The results of these experiments showed that the air flow oxidises the nuclear fuel and the ruthenium releases in form of volatile RuO_3 and RuO_4. One of the main results was that in the outlet air flow reaching the environment the partial pressure of RuO_4 was in the range of 10^{-6} bar, which is far above what would be expected for room-temperature equilibrium conditions. It was also observed the presence of other fission product elements in the nuclear fuel influenced the release rate of gaseous ruthenium.

It is well known that ruthenium in irradiated UO_2 appears in form of small alloy precipitations together with Mo, Rh, Pd and Tc (white inclusions). Present year's task was to study the differences in the release rate of gaseous ruthenium oxides when pure ruthenium metal or Mo-Ru-Rh-Pd metallic alloy is present in the simulated nuclear fuel.

The chemical composition of the alloy was determined based on literature data for spent PWR fuel with a burnup of 36.2 GWd/tU [4]. Technetium was not involved in the study because our laboratory works with non-radioactive materials. The experimental method was the same as in the RUSET-1 experiment [1]. The oxidation and release were studied at constant reaction temperatures of 1000 ºC or 1100 ^{o}C.

2. Experimental

2.1 Oxidation setup and sampling

The scheme of experimental facility is shown in Figure 1. The high temperature conditions on the sample were established in a vertical furnace. The furnace had three independently heated sections jointly controlled by a microprocessor that resulted in a 150-mm long, stable temperature zone in the middle; the temperature accuracy was 1-2 ºC. The reaction chamber is a quartz tube with a larger diameter part in the middle; it contains the test sample. The top of the quartz tube was connected with a Pyrex glass tube to the absorber device (bubbler).

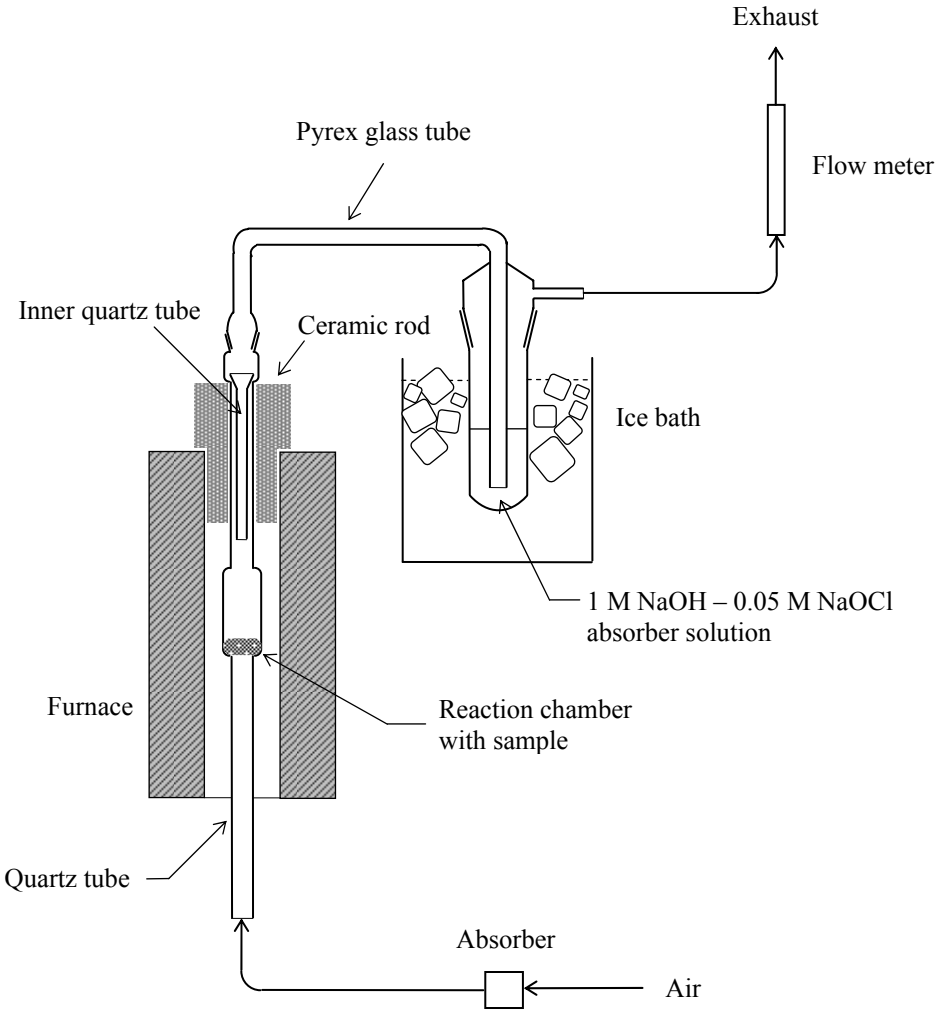

Figure 1: Scheme of the experimental facility

The experiments were carried out on samples prepared as a mechanical mixture of ZrO_2 powder and powdered Mo-Ru-Rh-Pd alloy. Some samples contained additional fission product elements. The selected concentrations of the powdered alloy (Mo 47% / Ru 27% / Rh 7% / Pd 19% by weight) and of the additional inactive fission product components represented a spent nuclear fuel of medium burnup, see Table 1. The samples contained the characteristic fission products including both volatile and non-volatile species. Similar composition was used in the SASCHA experiments at FZK [5].

In our tests, 1 g ZrO_2 with ~ 18.52 mg powdered alloy containing 5.0 mg Ru was prepared as sample and put into the reaction chamber. The air flow rate was maintained at 171.0 cm^3/min measured at room temperature. The release of gaseous Ru was fast enough to get equilibrium partial pressures for ruthenium oxides at this flow rate. During the tests, the air injection was started when the furnace with sample was heated up to the required isothermal temperature (to 1000 ºC or 1100 ºC). These two temperatures were chosen because at lower temperatures the release rates would be very low resulting in long measurement times, while above 1100 ºC the lifetime of quartz tubes would be too short and their deformation would happen.

Table 1: Composition of inactive fission product species representing a 44-GWd/tU burnup.

Compound	**Mass for 100 g charge [mg]**
CsI	72.10
Cs_2CO_3	408.45
Se	5.94
Sb	2.46
Cd	13.56
Te	70.59
Sn	7.27
Ag	7.68
Nd_2O_3	1111.68
CeO_2	406.24
$BaCO_3$	436.75
ZrO_2	570.79

During the experiments the released Ru was collected in two places; in an inner quartz tube placed into the outlet tube of reaction chamber and in a room temperature absorber solution (bubbler) at the outlet of circuit line.

When the temperature of air stream is decreasing from that of the furnace to the ambient level the $RuO_3 \leftrightarrow RuO_2 + 1/2\ O_2$ and $RuO_4 \leftrightarrow RuO_2 + O_2$ equilibrium chemical reactions shift towards the formation of RuO_2. The latter appears as deep blue precipitations on the quartz tube wall. In order to determine the amount of deposited RuO_2 and because of the difficulties with its solubility, an inner quartz tube was placed into the outlet tube of the reaction chamber in the decreasing temperature area. The upper end of the heated area was closed with a 65-mm-long ceramic rod with a hole in the middle at the outlet tube of the reaction chamber. The aim of this arrangement was to get a reproducible, decreasing temperature profile to determine the precipitated/deposited mass as a function of temperature and time. The decreasing temperature profile was measured with thermocouple and the results are plotted in Figure 2.

To quantify the gaseous ruthenium oxide components in the outlet gas flow after cooling down they were absorbed in alkaline hypochlorite solution (1 M NaOH – 0.05 M NaOCl) in the septivalent (perruthenate) form. To improve the efficiency of absorption the absorber solution was cooled in ice bath suggested by Larsen and Ross [6].

Both the inner quartz tube and the absorber solution were changed for a new one at the same moment, in all, 5 or 7 times in the tests conducted at 1100 ºC or 1000 ºC, respectively. This method gave the possibility to evaluate the RuO_x release from the furnace as a function of time.

In two experiments, where the charge contained additional compounds modelling fission products, a 2-mm-diameter quartz rod was placed into the first inner quartz tube. The outer surface of quartz rod is convenient for investigations with XRF and SEM methods to clarify the thermo-chromatographic effects.

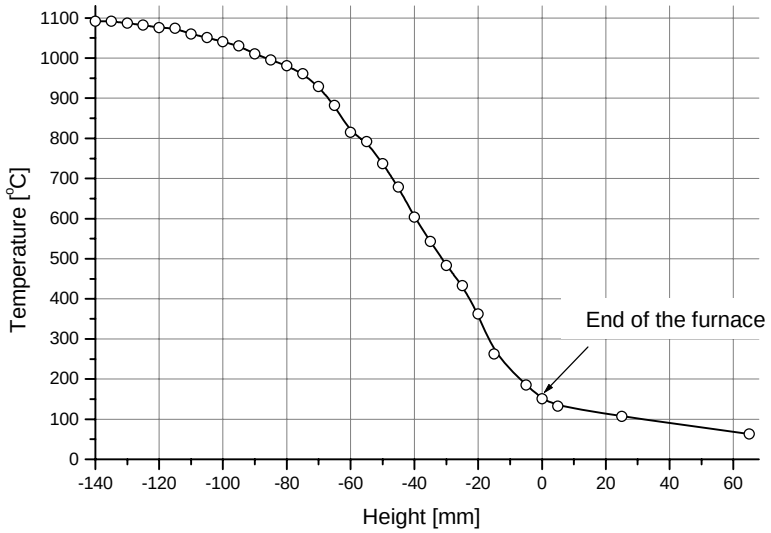

Figure 2: Thermal gradient at the upper end of vertical furnace (ceramic rod)

2.2 Determination of ruthenium total mass deposited in inner tubes

The mass of precipitations was measured by weighing of the inner quartz tubes before and after their use to get information about the total weight of volatilized and deposited components in a given sampling period. It reflects the amount of ruthenium if no other fission product than Ru is present.

The determination of amounts of ruthenium deposited in the inner quartz tubes was a sophisticated problem. As it was mentioned earlier in the decreasing temperature part of the reaction chamber RuO_2 is precipitated as a result of $RuO_3 \leftrightarrow RuO_2 + 1/2\ O_2$ and $RuO_4 \leftrightarrow RuO_2 + O_2$ chemical reactions. The RuO_2 is an exceptionally stable species. A direct dissolution would be troublesome (in hydrogen fluoride, melting with alkalis, etc.). However, the metallic ruthenium is soluble in alkaline hypochlorite solution.

Based on numerous pre-experiments to reduce the RuO_2 precipitated in the inner quartz tubes to Ru quantitatively a 5-hour heat treatment at 1100 ºC in $5\%H_2 + N_2$ gas stream proved to be appropriate. The formed metallic ruthenium was dissolved in alkaline hypochlorite solution and this solution was used directly for spectrophotometric measurements. The details of determination of Ru mass dissolved in the above-mentioned solution are given in section 2.3.

The surfaces of quartz rods placed inside the inner quartz tubes were investigated with SEM and XRF methods. The methods of these measurements are given in sections 2.4 and 2.5.

2.3 Determination of ruthenium content in absorber solutions

The basic method employed in our laboratory was the spectrophotometric determination. After numerous experimental efforts finally the method developed by Larsen and Ross at Argonne NL [6] has been found to be the most convenient. In this method,

perruthenate is the species to be measured in alkaline solution containing hypochlorite with low concentration. If the alkaline concentration is about 1 M and the hypochlorite is 0.05 M the ruthenium is in septivalent form (perruthenate) and stable for many days. Our results confirmed their published reproducibility.

The sensitivity of this method slightly lower than that of the others, but the long time stability is far more advantageous. The concentrations of alkaline and hypochlorite are allowed to be in a fairly broad range. The hypochlorite should be between 0.1 M and 0.01 M. Without hypochlorite a slow reaction towards ruthenate (sexivalent state) formation makes the colour of solution unstable, in case of too much hypochlorite a slow escape of RuO_4 takes place. According to our experiences the change of colour does not exceed 0.3 %/day in terms of concentration values and the found molar absorbance was in good agreement with the one published in [6].

Because in the perruthenate the Ru does not form complexes it is not necessary to keep very strict concentration values and time sequence, therefore the preparation of samples for spectrophotometric tests is definitely easier.

The absorption vessels contained ~ 20 ml 1 M NaOH – 0.05 M NaOCl solutions. The ruthenium concentrations of absorber solutions were measured without any further treatment by a MOM Spektromom 195D UV-VIS instrument using Quartz SUPRASIL cells of 1-cm length.

In Figure 3, the wavelength dependence of absorbance (A = - lg T) is shown for a reference perruthenate solution prepared from metallic ruthenium powder after 48 hours. The maximum value of absorbance is at 380 nm. The spectrum indicates that ruthenium is in perruthenate form [6].

The calibration of spectrophotometer has been made by metallic ruthenium powder dissolved in 1 M NaOH – 0.05 M NaOCl. The results are plotted in Figure 4.

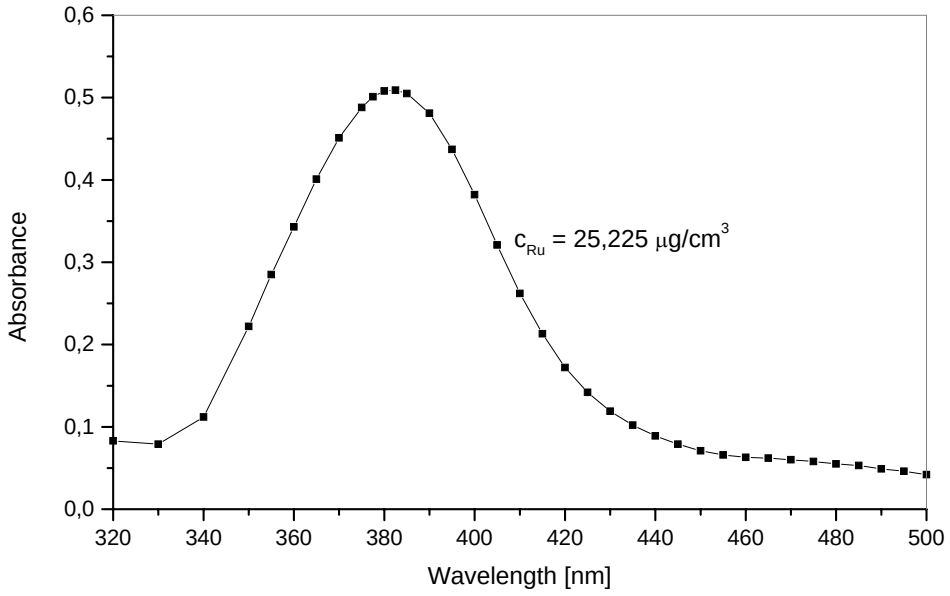

Figure 3: The absorbance spectrum of solution 48 hours after its preparation (ruthenium (VII) in 1 M NaOH – 0.05 M NaOCL)

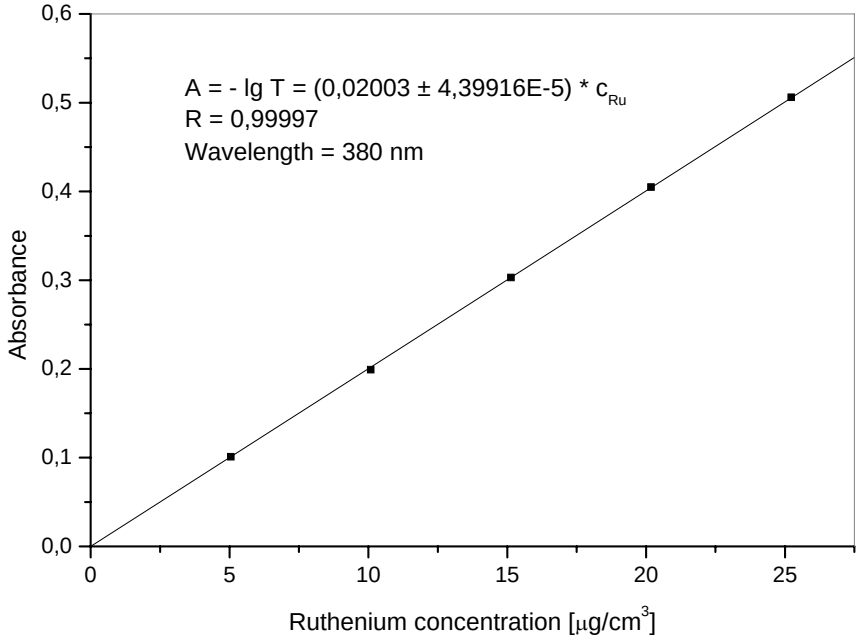

Figure 4 Dependence of light absorption on Ru-concentration measured at 380 nm in the standard perruthenate solutions

2.4 Electron probe microanalysis and methods

We applied the following instruments and methods:

1. Philips SEM 505 scanning electron microscope (SEM) working at 20 or 25kV and with a few nanoamper beam current. First we made secondary electron images (SEI) at 10-times magnification to see the overall view of the sampler rod segments. Then the both ends and the middle parts of the rod segments were studied at 300-times magnification. Some individual grains – crystals were detected at higher magnifications in the digital secondary electron images.
2. LINK AN 10/55 S type energy dispersive electron beam microanalyser (EDX) with a detection limit of few tenth of mass % in the elemental range between Na^{11} and U^{92}. The EDX measurements were done mostly at 300-times magnification at the ends and the middle parts of the rod segments. Some individual particles and aggregates were also analysed.
3. Oxford INCA EDX system with thin inlet window made it possible to detect elements from B^5 to U^{92}. We made quantitative EDX studies as well; however, the Si peak coming from the quartz rod material was always present. The amount of the Si detected depended on the coverage of the rod segments by deposits. High degree of deposition resulted in elements detected mostly in the deposited particles/layer, while sporadic deposition resulted in high amounts of Si originated from the rod segment as a substrate.

The sample preparation was simple: we cut a 52.2-mm-long section of the rod, where any deposition can be seen, into four segments. The length of segments was 14, 11, 12 and 15.2 mm, respectively. These segments were put onto a SEM specimen holder by means of double-sided carbon tape. To decrease the electrical charging effects, a thin carbon layer was sputtered on the surface of segments and they were numbered from 1 to 4.

2.5 Micro-beam X-ray fluorescence (μ-XRF) technique

In order to determine the axial distribution of the fission elements deposited along the sampler rod, the samples were investigated using micro-beam X-ray fluorescence (μ-XRF) technique. During the measurement the sample was scanned through a microscopic X-ray beam generated by a silver-anode fine-focus X-ray diffraction tube. The beam was focused to an 80-μm-diameter spot by means of a polycapillary mini-lens (IfG, Germany). The X-ray tube was operated at a high voltage of 50 kV and a current of 30 mA. The sample was fixed to a computer-controlled sample stage vertically and was moved in front of the capillary in vertical direction. Because of the relatively small vertical range of the movement, the original sampler rod was cut to 25-mm-long sections. The measurements were carried out in 1-mm steps; each point was measured during 100 seconds. The first measurement point was taken close to the hottest end of the sampler rod. The spectra were recorded by a Si (Li) X-ray detector and the intensities of the characteristic X-ray lines were evaluated by the AXIL code. Mo and Ru were determined by using K lines, while Cs and Te by L lines.

The relative sensitivities for the lines of interest (Mo-K_α, Ru-K_α, Cs-L_α, Te-L_α) were determined from measurements of thin standard samples of MoO_3, CsBr and ZnTe (Micromatter), as well as from a dried droplet prepared on a polypropylene X-ray film from Mo, Ru and Cs standard solutions (Spectrascan, 1 g/l and 5 μl each). The sensitivity coefficients relative to Ru-K_α were obtained as 0.81 for Mo-K_α, 0.88 for Cs-L_α and 0.72 for Te-L_α, allowing the calculation of relative masses of elements deposited on the sampler rod surface.

3. Results of measurements and discussion

3.1 Oxidation kinetics of ruthenium in the Mo-Ru-Rh-Pd alloy

In the frame of the present work six high temperature experiments with Mo-Ru-Rh-Pd alloy were performed to gain experimental data on the ruthenium oxidation from this alloy and to clarify any deviation in the oxidation rate from that of the pure metallic ruthenium powder. The results are summarized in Table 2, where the notations are as follows:

t	temperature in the reaction chamber
m_{Ru}	ruthenium content of the charge
sampling time	sampling time of a given sample
V_{air}	total volume of air streamed through the reaction chamber during a given sampling period
Δm	total weight of deposited components in the inner quartz tube at a given sampling period
$\Delta m_{precipitated}$	amount of ruthenium precipitated in the inner quartz tube
$\Delta m_{absorbed}$	mass of ruthenium absorbed in alkaline hypochlorite solution
$p_{furnace}$	partial pressure of RuO_x in the reaction chamber
$p_{outlet\ air}$	partial pressure of RuO_x in the outlet gas after cooling down
$t_{equilibrium}$	temperature which would result $p_{outlet\ air}$ in equilibrium

The partial pressure of RuO_x in the high temperature reaction chamber was calculated from the total amount of precipitated and absorbed ruthenium, while the partial pressure of RuO_4 in the escaping ambient temperature gas was calculated from the amount of ruthenium captured in the absorber solution and the volume of gas streamed through during a given sampling time.

These partial pressure values are plotted as functions of time in Figure 5 and Figure 6. In Figure 5, the average values of parallel measurements at 1100ºC are given, while in Figure 7 these average values for alloy have been compared with those got in RUSET1 tests for pure ruthenium powder. The temperature values (t equilibrium), which would result the same partial pressures in equilibrium as measured in the escaping gas, were calculated using the equilibrium equations published in [7]. These equations are in good agreement with our earlier results [1] and with the measured and calculated values published in [8]. These equations are the followings:

for process $RuO_2(s) + O_2 \leftrightarrow RuO_4(g)$

$$\lg K_p = - 6219.4/T + 4.2120 - 1.0315 \lg T - 0.0557 \cdot 10^5 \cdot T^{-2} \quad (1)$$

for process $RuO_2(s) + ½\ O_2 \leftrightarrow RuO_3(g)$

$$\lg K_p = - 12968.5/T + 10.1385 - 1.2429 \lg T - 0.1399 \cdot 10^{-3}\ T + 0.033 \cdot 10^5 \cdot T^{-2} \quad (2)$$

with K_p [atm] and T [K].

Table 2: Results of ruthenium release experiments carried out with the Mo-Ru-Rh-Pd alloy

Main parameters	**Sample**	**Sampling time [min]**	**V air [dm^3]**	**Δm [mg]**	**Δm precipitated [mg]**	**Δm absorbed [mg]**	**P furnace [bar]**	**P outlet air [bar]**	**t equi-librium [^{o}C]**
t = 1100^{o}C	I-1	30	5.14	6.90	2.65	0.48	1.50E-04	2.32E-05	920.7
	I-2	30	5.14	1.74	1.14	0.21	6.51E-05	1.03E-05	858.8
Alloy	I-3	30	5.14	0.30	0.16	0.14	1.42E-05	6.78E-06	827.2
	I-4	30	5.14	0.02	0.03	0.03	3.12E-06	1.62E-06	721.3
m_{Ru}=5.12mg	I-5	30	5.14	0.12	0.00	0.00	2.40E-07	6.00E-08	528.6
t = 1100^{o}C	II-1	30	5.14	6.59	2.35	0.50	1.37E-04	2.38E-05	922.8
	II-2	30	5.14	1.31	0.67	0.28	4.56E-05	1.34E-05	879.0
Alloy	II-3	30	5.14	0.77	0.39	0.17	2.71E-05	8.22E-06	841.9
	II-4	30	5.14	0.37	0.20	0.12	1.51E-05	5.76E-06	814.8
m_{Ru}=5.09mg	II-5	30	5.14	0.11	0.03	0.13	7.62E-06	6.36E-06	822.3
t = 1100^{o}C	III-1	30	5.14	5.15	2.21	0.34	1.23E-04	1.64E-05	894.7
	III-2	30	5.14	1.04	0.57	0.55	5.36E-05	2.62E-05	929.9
Alloy + FP	III-3	30	5.14	0.43	0.17	0.38	2.68E-05	1.84E-05	903.4
	III-4	30	5.14	0.89	0.03	0.18	1.03E-05	8.76E-06	846.7
m_{Ru}=5.01mg	III-5	60	10.29	0.29	0.01	0.06	1.65E-06	1.53E-06	717.3
t = 1100^{o}C	IV-1	30	5.14	4.38	2.26	0.35	1.26E-04	1.70E-05	897.2
	IV-2	30	5.14	2.09	0.95	0.64	7.63E-05	3.06E-05	941.7
Alloy + FP	IV-3	30	5.14	0.79	0.17	0.36	2.54E-05	1.75E-05	899.3
	IV-4	30	5.14	0.23	0.01	0.07	3.84E-06	3.24E-06	771.5
m_{Ru}=5.05mg	IV-5	60	10.29	0.53	0.00	0.02	6.60E-07	5.70E-07	651.8
t = 1000^{o}C	V-1	60	10.29	4.96	0.89	0.64	3.68E-05	1.54E-05	889.7
	V-2	60	10.29	1.30	0.69	0.31	2.41E-05	7.50E-06	834.9
Alloy	V-3	60	10.29	0.69	0.38	0.30	1.64E-05	7.26E-06	832.4
	V-4	120	20.57	1.11	0.53	0.36	1.07E-05	4.27E-06	792.2
m_{Ru}=5.06mg	V-5	120	20.57	0.41	0.19	0.25	5.31E-06	3.00E-06	765.8
	V-6	120	20.57	0.07	0.05	0.16	2.56E-06	1.96E-06	735.0
	V-7	60	10.29	0.01	0.00	0.07	1.71E-06	1.62E-06	721.3
t = 1000^{o}C	VI-1	60	10.29	2.78	0.90	0.65	3.72E-05	1.56E-05	890.9
	VI-2	60	10.29	0.80	0.36	0.73	2.61E-05	1.75E-05	899.3
Alloy + FP	VI-3	60	10.29	0.46	0.17	0.63	1.90E-05	1.50E-05	887.9
	VI-4	120	20.57	0.48	0.13	0.75	1.05E-05	8.94E-06	848.3
m_{Ru}=5.04mg	VI-5	120	20.57	0.16	0.03	0.29	3.79E-06	3.46E-06	776.5
	VI-6	120	20.57	0.15	0.01	0.13	1.69E-06	1.60E-06	720.7
	VI-7	120	20.57	0.13	0.01	0.02	4.20E-07	2.85E-07	610.1

As it was mentioned above, for the determination of ruthenium content of materials precipitated in the inner quartz tubes a 5-hour heat treatment at 1100ºC in 5%H_2 + N_2 gas stream was used to reduce RuO_2 to Ru. This reduction process provided reliable results even in the presence of other deposited elements like Mo, Cs, and Te on the inner quartz tube. Moreover by application of Pyrex glass connecting tube instead of Teflon tube and alkaline hypochlorite absorber solution instead of diluted hydrochloric acid 90-95%, the ruthenium mass balance could be performed.

In case of pure alloy, the molybdenum oxidized fairly fast to MoO_3. After ten minutes as the air injection started polymer $(MoO_3)_n$ appeared as white aerosol. However this phenomenon was not observable when other fission product components were present in the charge. Presumably some compounds of the fission product elements prevented the initial intensive molybdenum release.

From the present results, it seems that the oxidation rate of ruthenium from Mo-Ru-Rh-Pd alloy is about 60% of the theoretical evaporation rate of pure ruthenium at 1000 and 1100ºC as well [8]. This slower reaction rate (70-80%) could be partly resulted by the larger grain size of the powdered alloy compared to that of the commercial ruthenium powder used in RUSET1 tests [1] (see Figure 7).

There were no significant differences in the partial pressures of RuO_x in the high temperature reaction chamber between the pure alloy and the alloy with other fission product components neither at 1100ºC nor at 1000ºC oxidation temperature (see Figure 5 and Figure 6). The calculated partial pressure of RuO_x [7], i.e. the oxidation rate of pure ruthenium in air is 3.7 times smaller at 1000ºC than at 1100^{o}C. The ratio of the measured partial pressures of RuO_x at 1100 and 1000ºC is 3.6.

In case of pure Mo-Ru-Rh-Pd alloy the concentration of RuO_4 in the ambient temperature outlet gas decreased continuously in time, while in presence of other fission product elements a time delay appeared like to earlier experiments conducted with ruthenium powder and other fission products [1]. In presence of other fission products the maximum concentration of RuO_4 in the outlet air appeared between 30 and 60 min at 1100ºC, and between 60 and 120 min at 1000ºC (see Figure 5 and Figure 6). On the other hand, there was no time delay in the escaping of ruthenium from the high temperature reaction area (partial pressure of RuOx in the furnace dropped continuously in time). This suggests that reactions in the outlet area with decreasing temperature delayed the release of ruthenium in the escaping cooled down air.

The total amount of Ru captured in alkaline hypochlorite solution was greater in case of tests performed at 1000ºC than at 1100^{o}C. This is due to the longer reaction (sampling) time, because the partial pressures of RuO_4 in the ambient temperature outlet gas in a given time period are quite the same at 1000 ^{o}C and 1100 ^{o}C as well (see Figure 8).

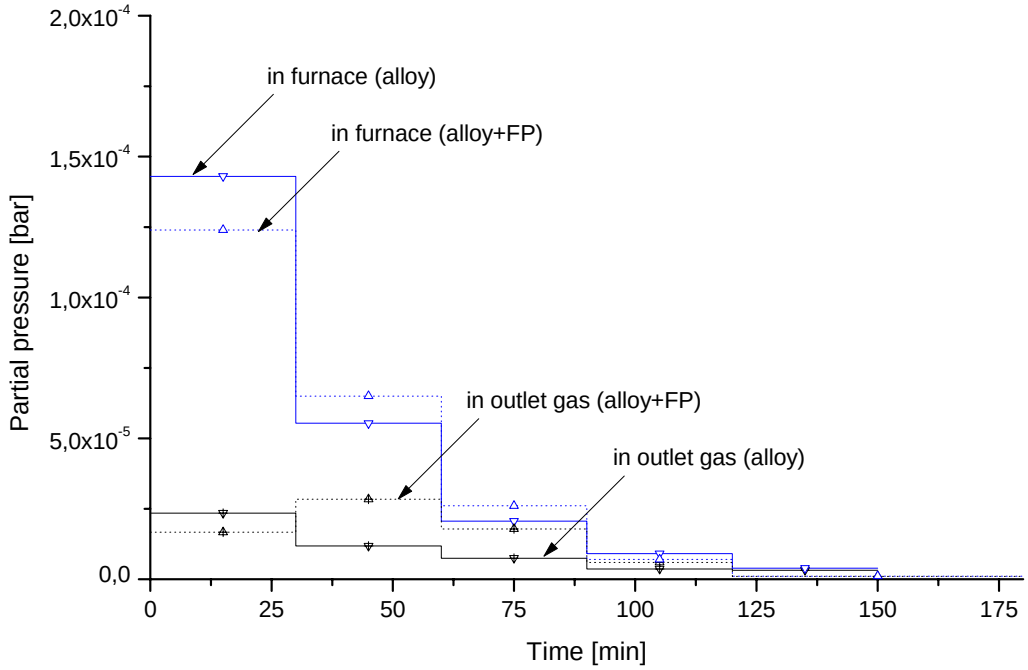

Figure 5: Partial pressure of ruthenium-oxides in the furnace (1100 ºC) and in the outlet air (room-temperature) as a function of time; outlet air flow is 171 cm^3/min.

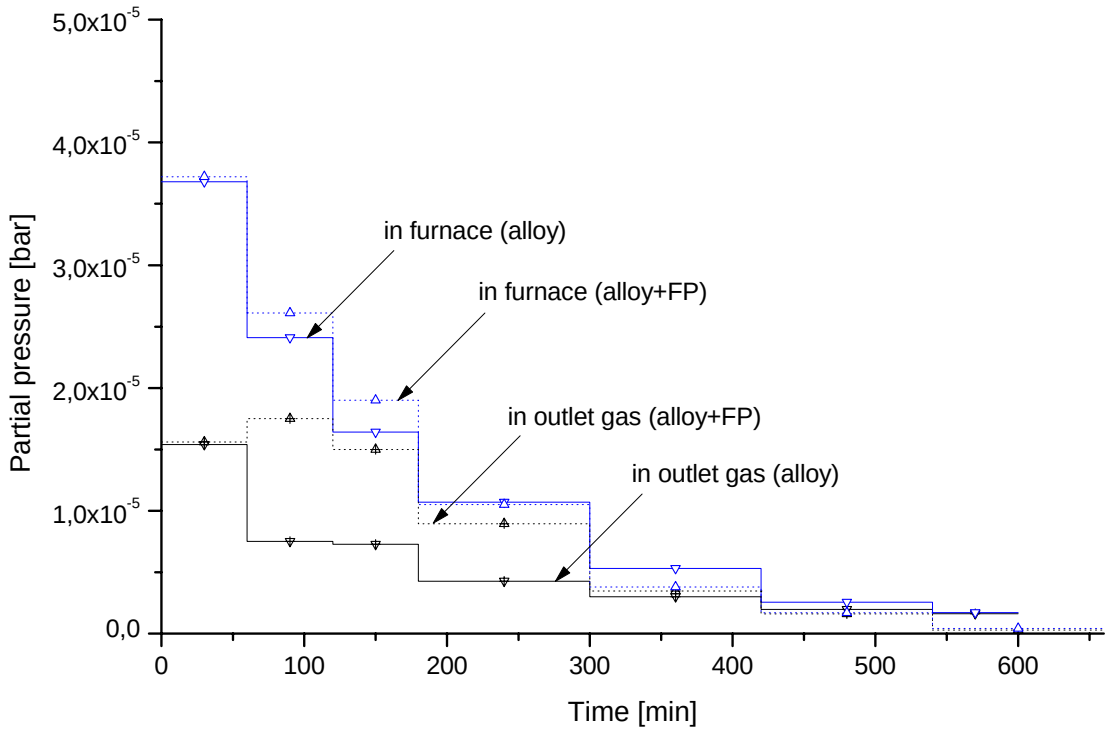

Figure 6: Partial pressure of ruthenium-oxides in the furnace (1000 °C) and in the outlet air (room-temperature) as a function of time; outlet air flow is 171 cm^3/min.

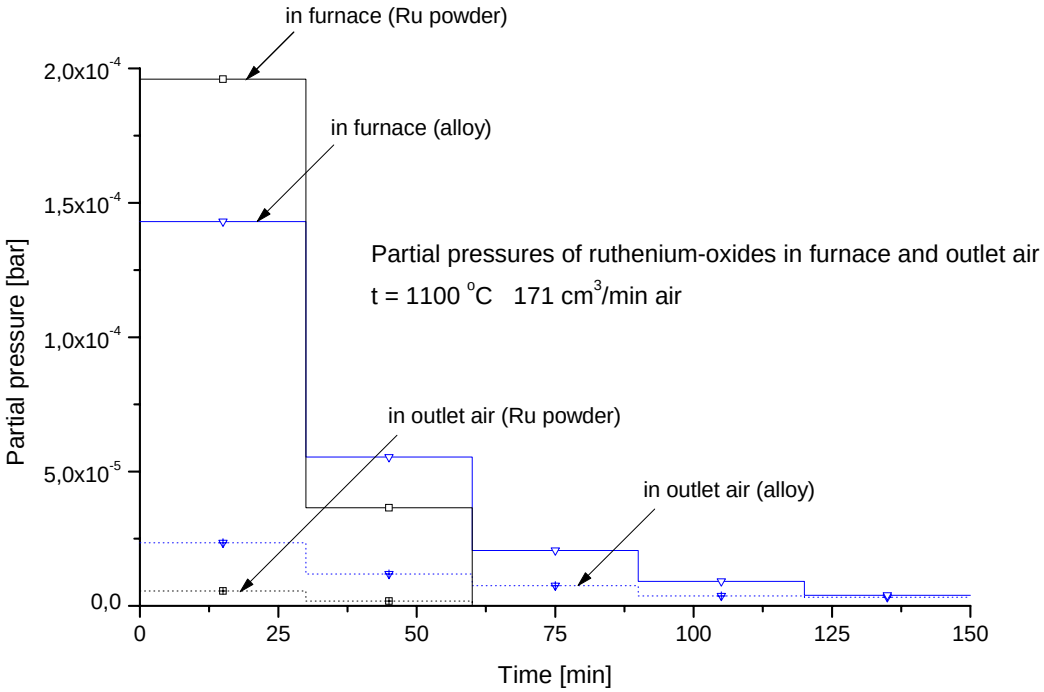

Figure 7: Comparison of the oxidation of pure Ru and of the Mo-Ru-Rh-Pd alloy at 1100 °C both dispersed in ZrO_2 powder as a matrix.

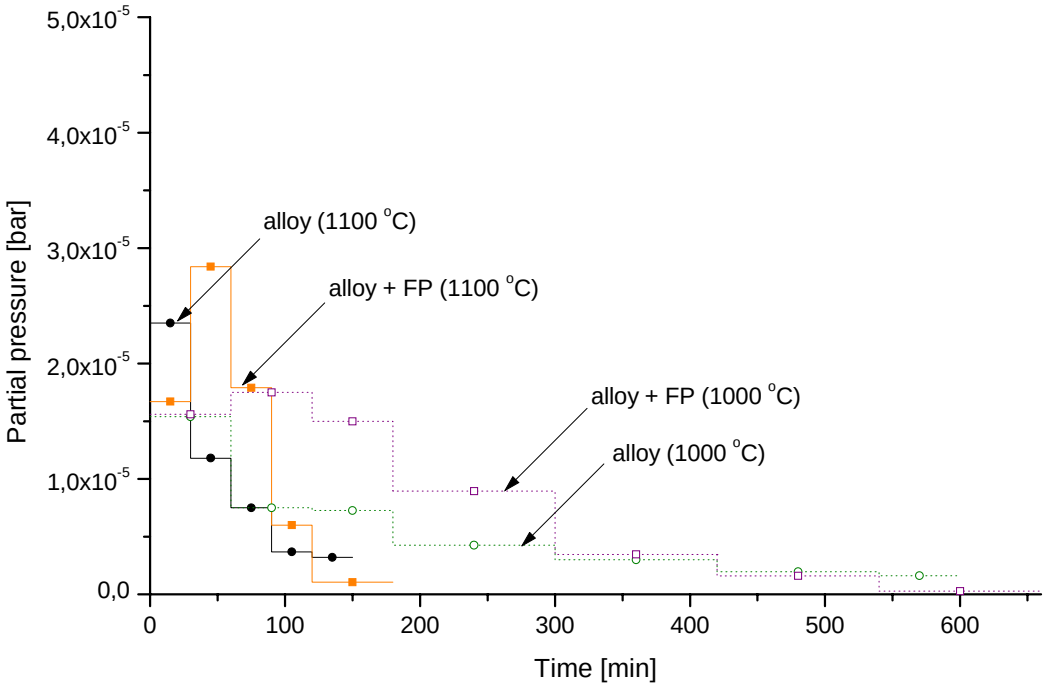

Figure 8: Partial pressures of gaseous ruthenium-oxides in the ambient-temperature outlet air flow of 171 cm^3/min.

3.2 XRF analysis of deposition profile of elements on quartz rod (Sample VI-1)

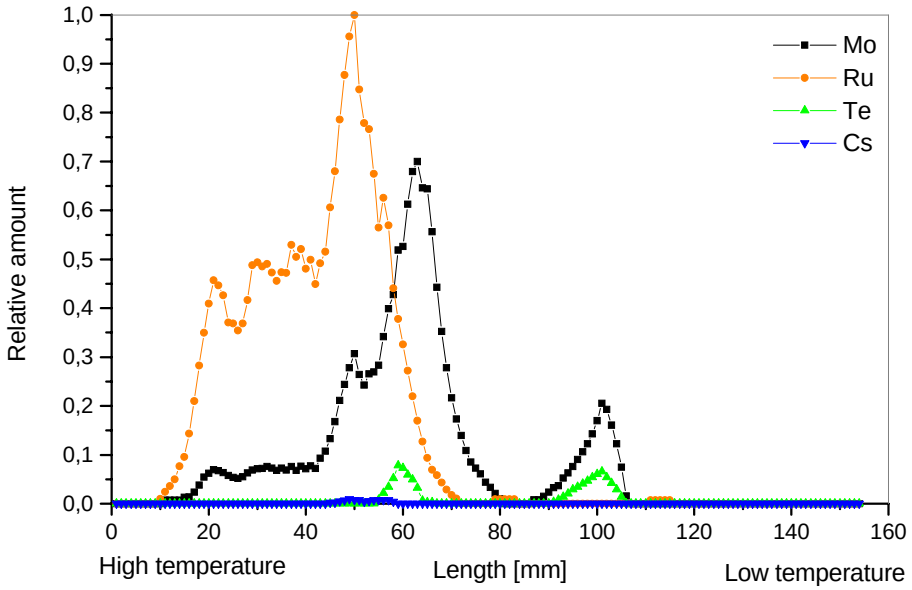

Figure 9: Axial distribution of deposited elements along the sampler rod VI-1.

The axial distribution of deposited elements (see Figure 9) on the vertical quartz rod (sample VI-1, t=1000 ^{o}C) shows the thermo-chromatographic effect clearly. The zero length coordinate corresponds to the high-temperature end of the rod. Because of the longer sampling time (60 min) the elements got separated in an efficient way along the investigated quartz rod. The second peak at about 100 mm should correspond to a deposited compound with a 2:1 Mo:Te ratio.

3.3 Electron beam studies of particles deposited on quartz rod (Sample III-1)

The aim of the electron beam studies was to study the morphological features and the elemental composition of particles/layers deposited on the sampler rod no. III-1. By these studies we can see the differences in deposition of various fission elements as a function of rod temperature.

In Figures 10a and 10b digital SEI images taken at 10-times magnification show the different segments of the sampler rod no. III-1. In Figures 10a and 10c the lowest rod segment is no. 1, above it there are the other segments, no. 2-4. In Figures 10b and 10d the lowest rod segment is the no. 3, above it there were rod segments no. 2 and 4.

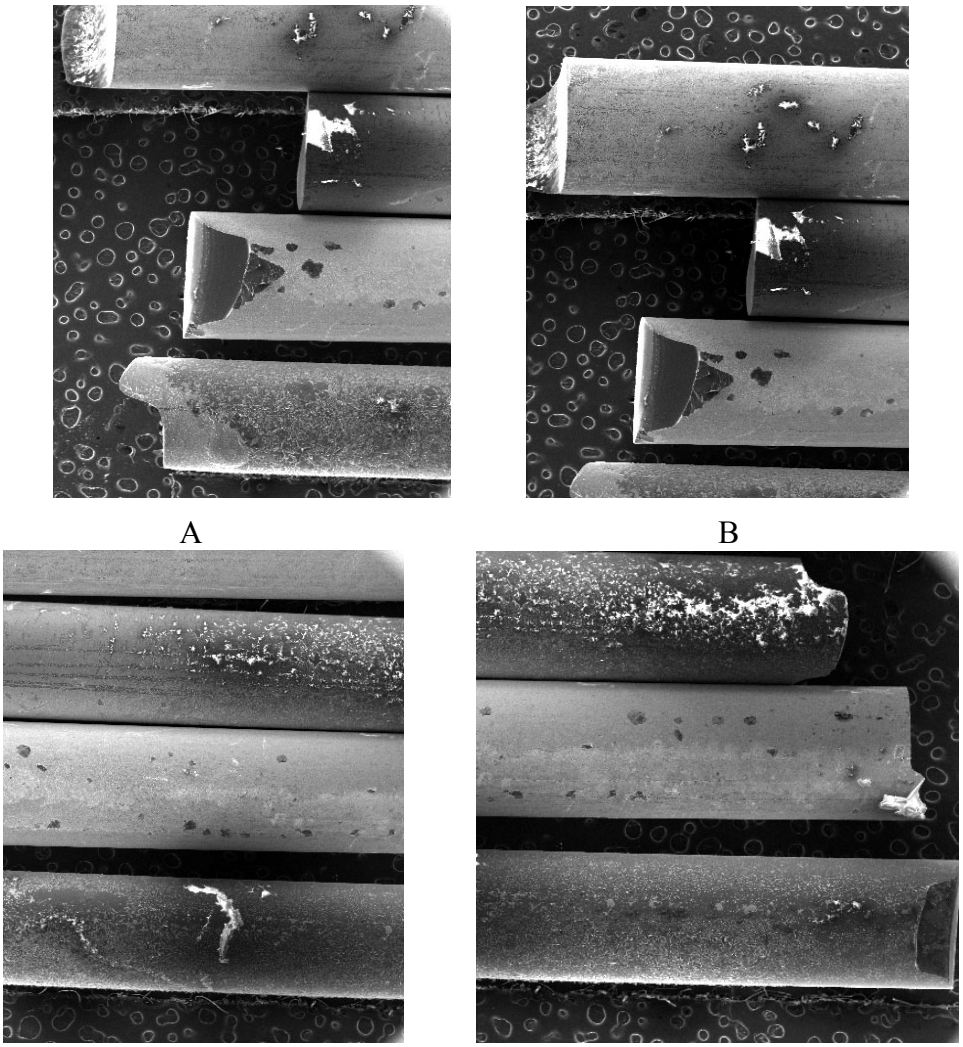

A B C D

Figure 10: Digital SEI images of segments of the rod no. III-1

There were particles and aggregates on each rod segment; however the coverage was various. Rod segment no. 1 was at the lower temperature part of rod no. III-1, while rod segment no. 4 had the highest temperature. On rod segment no. 1 smaller degree of deposition could be found than on rod segment no. 4. Some defects probably due to the cutting of the rod and its handling could also be seen.

All these features could be more easily recognized in the images taken at 300-times magnification; see Figure 11 through Figure14. Here the images on the left/right hand side correspond to the low/high temperature part of the rod segments; whereas the middle image to their middle part.

Lower temperature end Middle part Higher temperature end

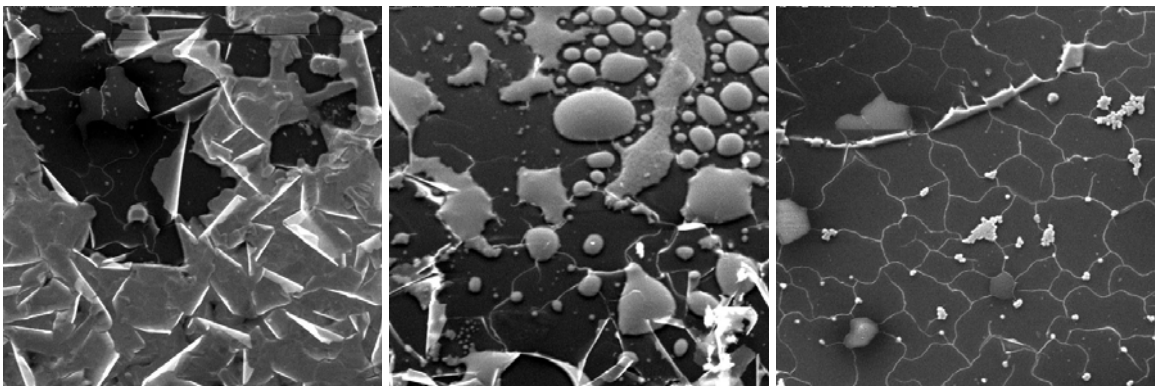

Figure 11: Typical SEI images of rod segment no. 1 of rod III-1 (200 μm x 200 μm areas)

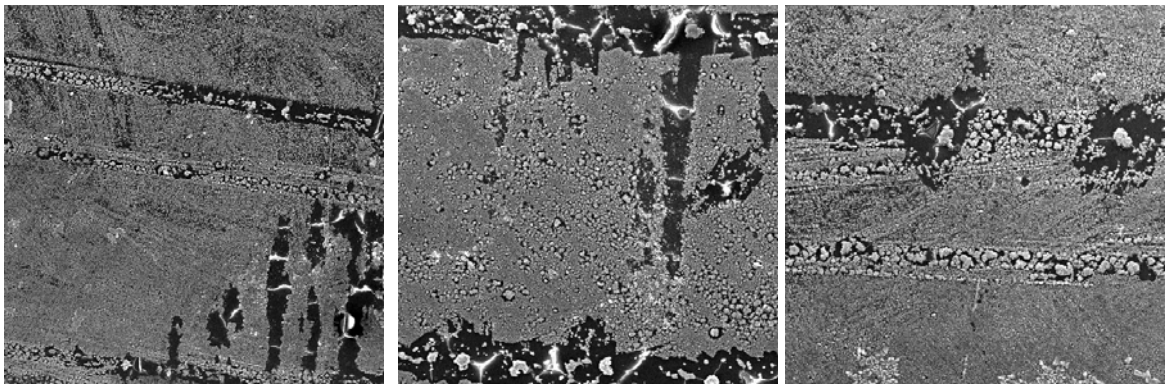

Figure 12: Typical SEI images of rod segment no.2 of rod III-1 (200 μm x 200 μm areas)

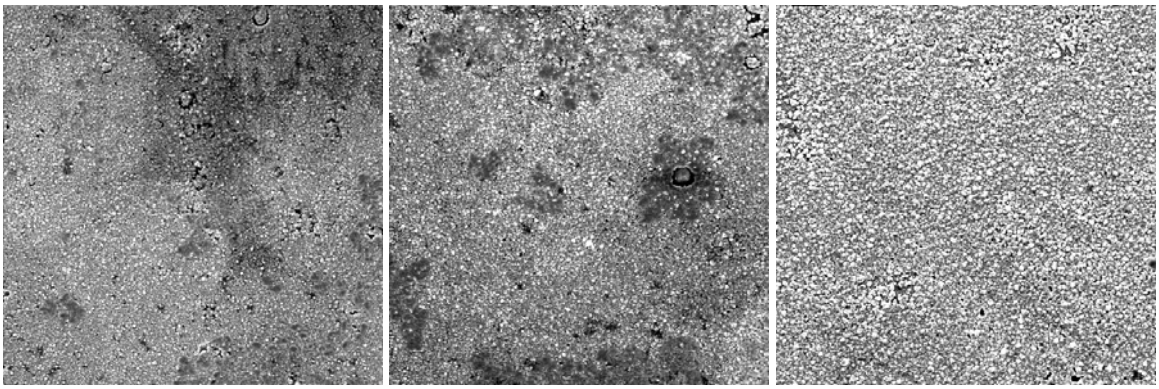

Figure 13: Typical SEI images of rod segment no. 3 of rod III-1 (200 μm x 200 μm areas)

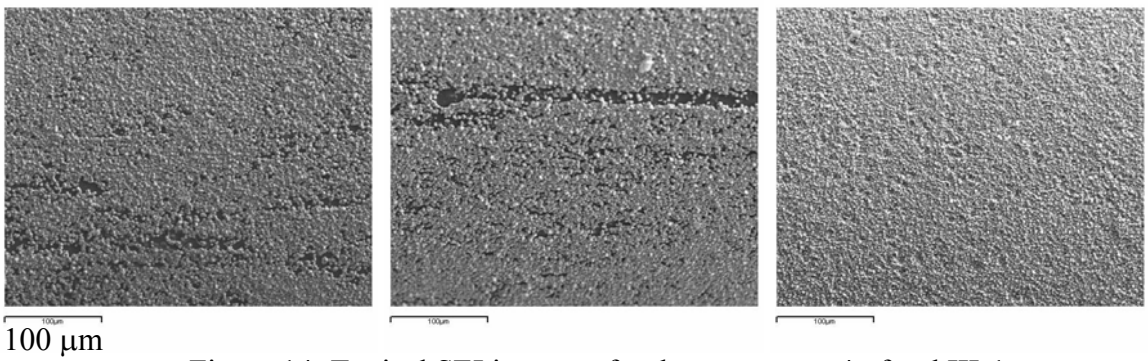

Figure 14: Typical SEI images of rod segment no. 4 of rod III-1

It can be concluded from the presented images that the coverage of the sampler rod by deposits decreased as the temperature decreasing along the rods. At the lower-temperature side

of the rod (segment no. 1) larger plates and mostly globular or slightly irregular crystallites could be found (see Figure 15).

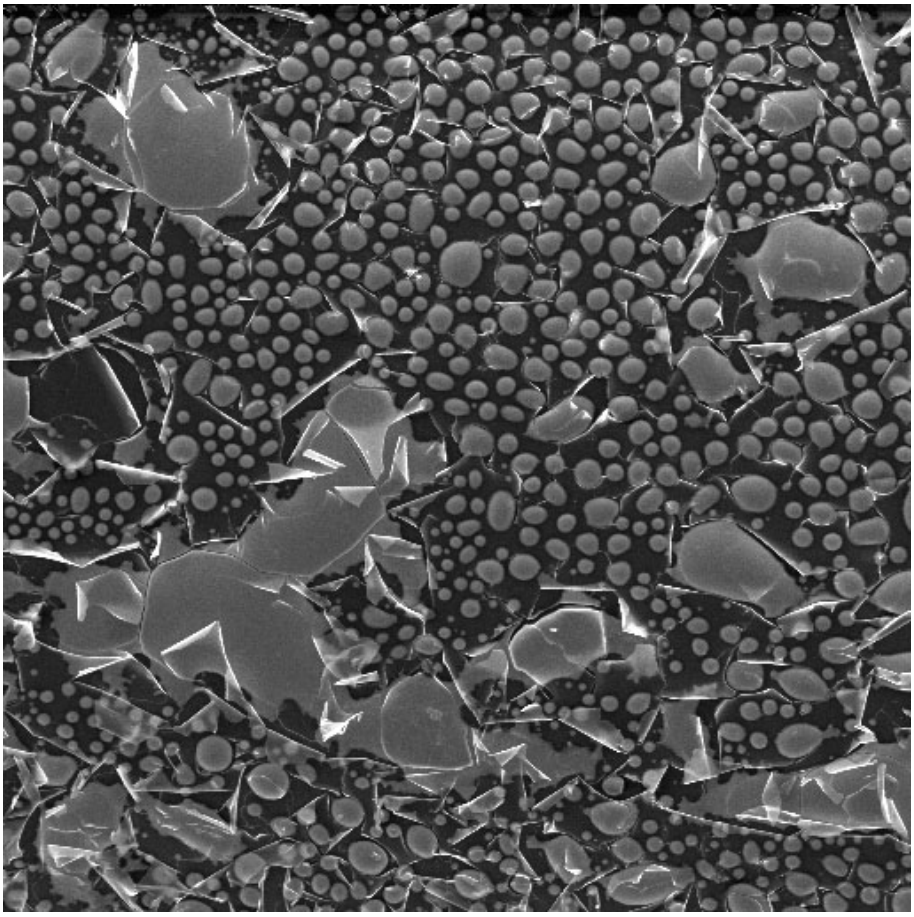

200 μm x 200 μm area

Figure 15: Larger irregular and smaller globular-elongated grains at the low-temperature side of sampler rod no. III-1 (segment no. 1)

The size of the globular crystallites varied between 2 and 8 μm, while the larger irregular grains had sizes of 10 to 40 μm. The elemental analysis revealed that both size types have Te, Mo and O content depending on the size; and Si was also present from the rod material.

Figure 16a and 16b show the typical ED spectrum taken from the lower/higher temperature end of rod segment no. 1, correspondingly.

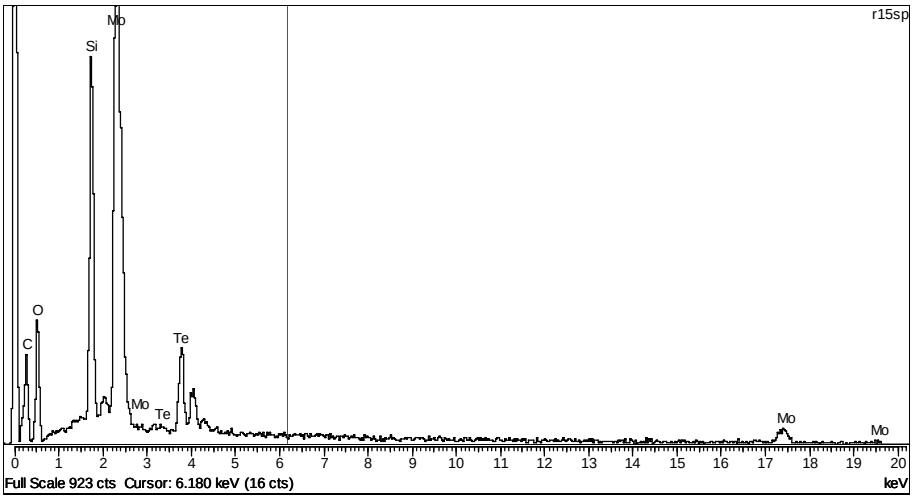

A: lower temperature end

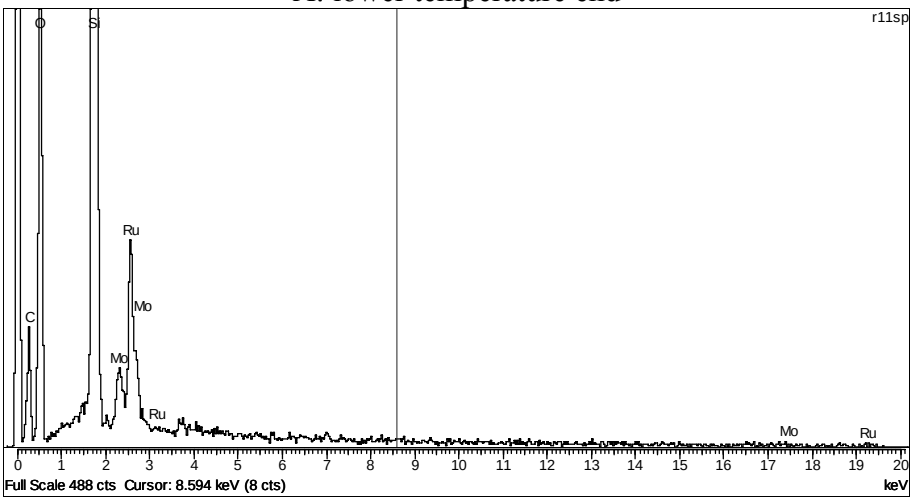

B: higher temperature end

Figure 16: Typical ED spectrums taken at low/high temperature end of rod segment no. 1.

By proceeding along rod segment no. 1 towards increasing temperatures Ru began to appear and the amounts of Te decreased. Aggregates on the right hand side image of Figure 11 were enriched in Ru with small amounts of Te and Mo, while the long plate-like structure had Te and Mo content.

Rod segment no. 2 had higher degree of deposition than rod segment no. 1, and the most important component elements were Ru, O, and in smaller amounts, Mo.

Rod segment no. 3 had even higher degree of deposition with Ru, Mo, O and Cd content. The higher degree of deposition is evident from the presence of very small Si peak originating from the rod material as a substrate. Figure 17 shows a digital SEI image taken at higher magnification (1200 times); while Figure 18 shows the ED spectrum registered in the middle part of this SEI image.

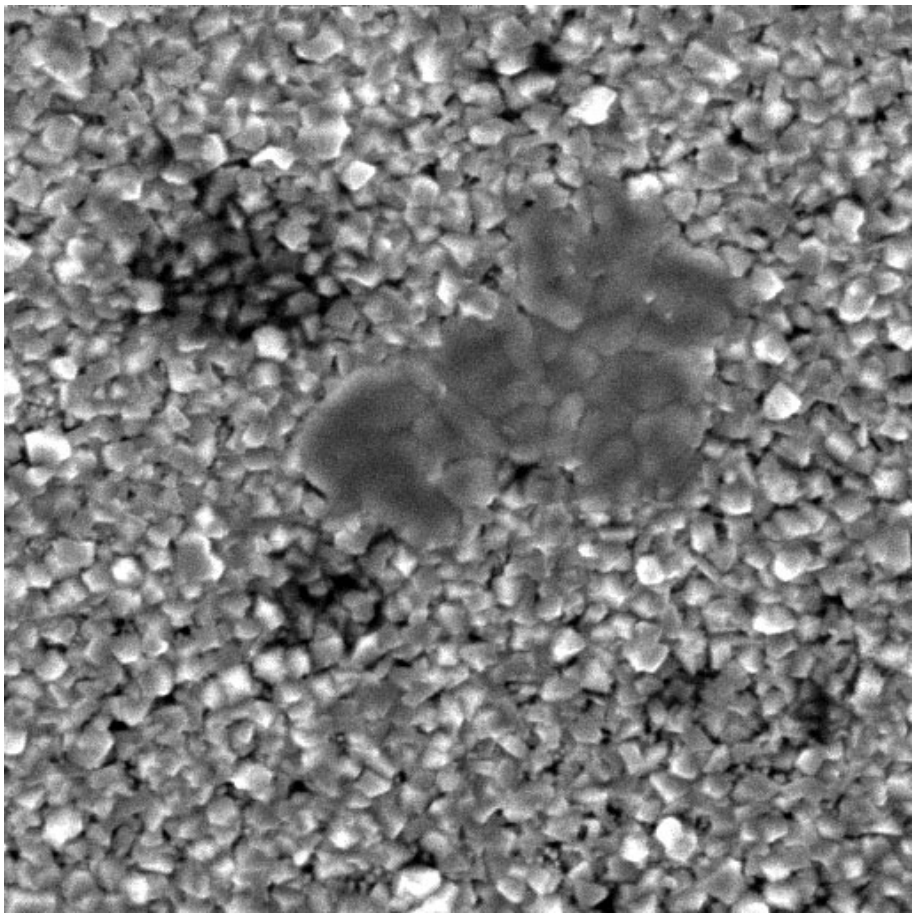

50 μm x 50 μm area

Figure 17: Digital SEI image at middle part of rod segment no. 3 from sampler rod III-1

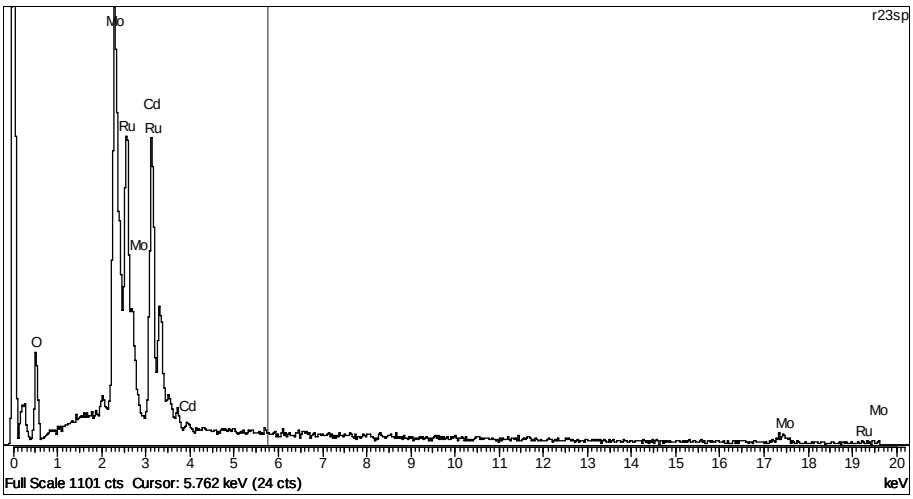

Figure 18: ED spectrum at middle part of rod segment no. 3 from sampler rod III-1

When moving towards locations with higher temperatures, high degree of deposition and much Ru could be found. This is especially true for sample segment no. 4. Figure 19 shows the middle part of this segment, where almost evenly distributed crystallites with 2 to 4 μm size could be revealed. It could also be seen that these crystallites formed aggregates as well. Figure 20 shows a typical ED spectrum of sample segment no. 4, where Ru, O and small amounts of Si can be seen.

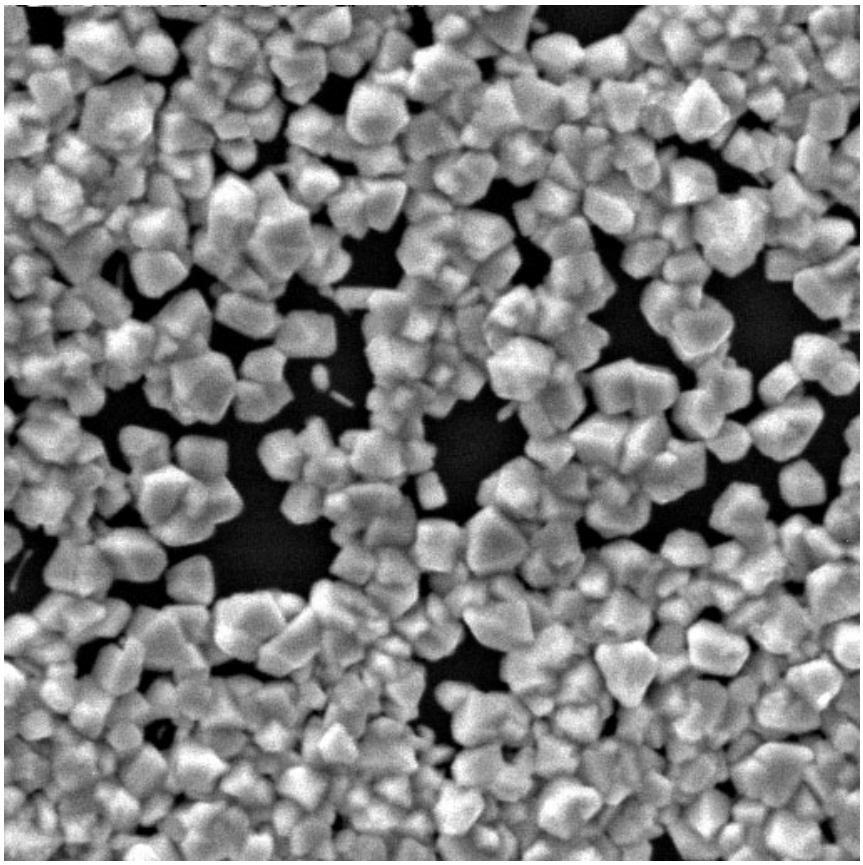

50 μm x 50μm area

Figure 19: Digital SEI image taken at middle part of rod segment no. 4 from sampler rod III-1

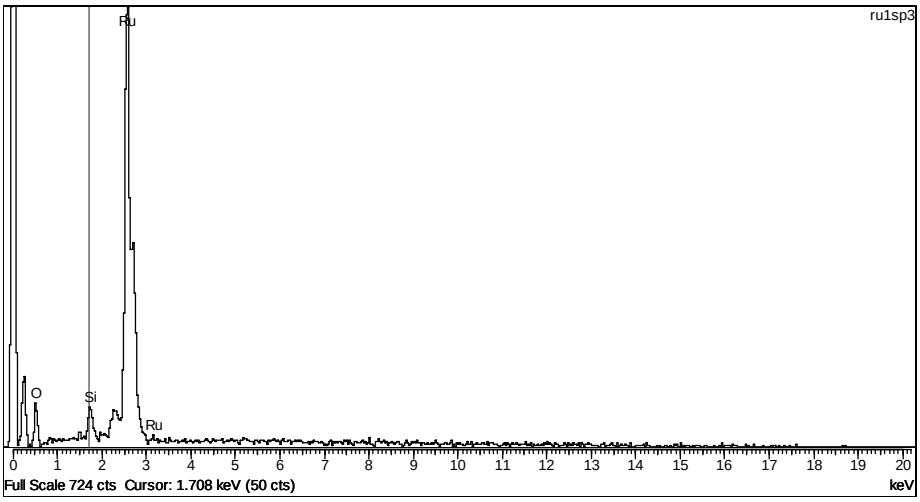

Figure 20: Typical ED spectrum of rod segment no. 4 from sampler rod III-1

Figure 21 summarizes the results of EDX measurements taken at the ends and in the middle parts of the four segments of sampler rod no. III-1. The zero length coordinate

corresponds to the high temperature part of the segment, while toward the 52.2-mm coordinate the temperature decreases.

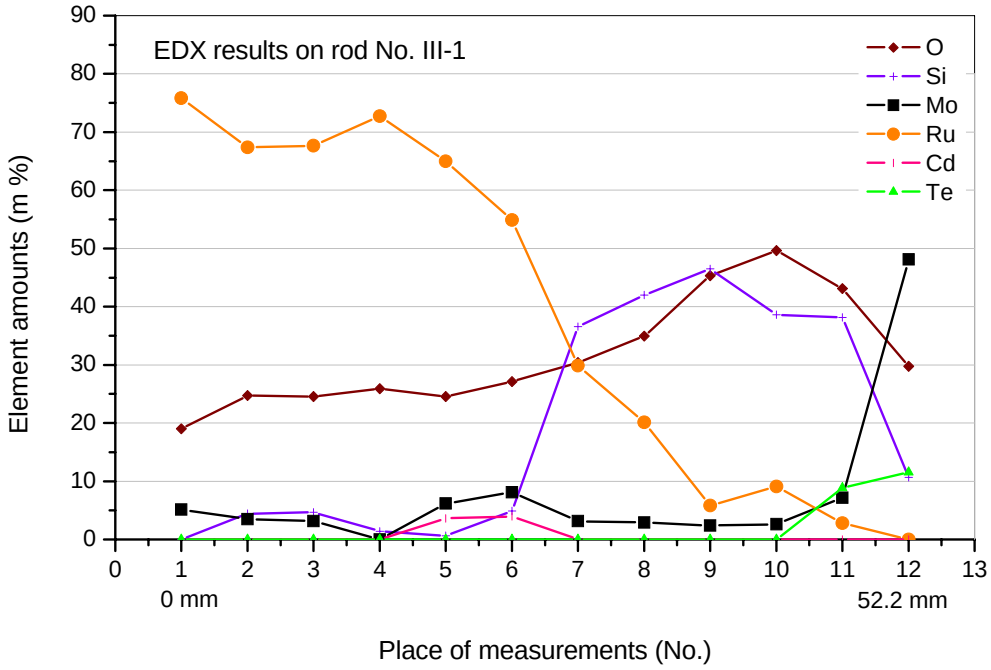

Figure 21: Summarized EDX results measured on the segments taken from the bottom of sampler rod no. III-1

Summary of EPMA studies

Electron beam studies (SEM and EDX) were performed on the segments taken from rod no. III-1. The degree of deposition along the rod changed from sporadic to highly dense as a function of the rod temperature. At the lower temperature part of the rod irregular large and smaller sized globular and elongated grains were found, which contained Te, Mo and O (and also Si coming from the rod material as a substrate). Toward the higher temperature part, small sized globular grains, and then crystallites with definite forms were detected, which contained mostly Ru and O. Further moving along the rod to higher temperatures, smaller amounts of Mo, Te and Cd could be found. In general, the spatial distribution of deposition of various elements representing the fission products was similar to the findings of the AEKI experiments performed earlier [3].

4. Conclusions

During high temperature oxidation of Mo-Ru-Rh-Pd alloy in air flow the escape rate of gaseous ruthenium oxides is reduced to 60-80% compared to the value measured in case of oxidation of pure metallic ruthenium powder in the same thermal-hydraulic conditions.

In the high temperature reaction chamber, there were no significant differences in the partial pressures of RuO_x when pure alloy or an alloy with additional fission product components was oxidized. The measured and calculated [7] ratio of the partial pressure of RuO_x at the reaction temperature of 1000 ^oC and 1100 ^oC agreed well.

If additional fission products were present in the alloy a time delay appeared in the release of gaseous ruthenium to the room-temperature environment similarly to earlier experiments conducted with the mixture of ruthenium powder and fission products. This delay was about 30 min at 1100 ^oC and about 60 min at 1000 ^oC. However, there was no delay in the release of ruthenium to the high temperature reaction area at the outlet of furnace.

The probable cause of the delay is chemical reactions on the surfaces of outlet circuit where the temperature gradually decreases to room temperature at the circuit outlet. Furthermore, molybdenum oxide and other fission product elements deposited in the inner quartz tube decrease the catalytic effect of quartz to form solid RuO_2. Therefore the amount of Ru captured in the absorber solution was greater during the oxidation of pure alloy and of the alloy with additional fission products than in tests conducted with metallic ruthenium powder.

5. References

[1] L. Matus, O. Prokopiev, B. Alföldy, A. Pintér, Z. Hózer: Oxidation and release of Ruthenium in high temperature air, Document PHEBUS PF: HU-02-1, AEKI (2002)

[2] L. Matus, I. Nagy, P. Windberg, N. Vér, M. Kunstár, B. Alföldy, A. Pintér, Z. Hózer: Oxidation and release of Ruthenium from short fuel rods in high temperature air, AEKI-FRL-2004-111-01/01, AEKI (2004)

[3] I. Nagy, Z. Hózer, L. Matus, A. Pintér, P. Windberg, N. Vér, M. Kunstár, B. Alföldy: Oxidation and release of Ruthenium from short fuel rods above 1500^{o}C, AEKI-FRL-2005-264-01/01, AEKI (2005)

[4] C. H. Lee, M. Y. Suh, K. S. Choi, et al., Determination of Ru, Rh, Pd, Te, Mo and Zr in spent pressurized water reactor fuels by ion exchange and extraction chromatographic separations and inductively coupled plasma atomic emission spectrometric analysis Analytica Chimica Acta 475 (2003) 171-179.

[5] H. Albrecht, Freisetzung von Spalt- und Aktivierungsprodukten beim LWR-Kernschmelzen, Abschlussbericht des SASCHA-Programmes, KfK 4264 (1987)

[6] R. P. Larsen, L. E. Ross, Spectrophotometric Determination of Ruthenium, Analytical Chemistry 31 (1959) 176-178**.**

[7] H. Schäfer, A. Tebben, W. Gerhardt, Zur Chemie der Platinmetalle V. Gleichgewichte mit Ru(f), RuO_2(f), RuO_3(g) und RuO_4(g), Zeitschrift für anorganische und allgemeine Chemie 321 issue 1-2 (1963) 41-55.

[8] Wayne E. Bell, M. Tagami, High-Temperature Chemistry of the Ruthenium-Oxygen System[1], J. Phys. Chem. 67(11) (1963) 2432-2436.

European Commission

EUR 22730 EN – DG JRC – Institute for Energy
Oxidation and Release of Ruthenium from White Inclusions

Authors:
N. Vér[1)]
L. Matus[1)]
M. Kunstár[1)]
A. Pintér[1)]
J. Osán[1)]
Z. Hózer[1)]
B. Tóth[2)]

1) Hungarian Academy of Sciences, KFKI Atomic Research Institute
2) European Commission, Joint Research Centre,
Institute for Energy, The Netherlands

Luxembourg: Office for Official Publications of the European Communities
2007 – 27 pp. – 21 x 29.7 cm
EUR - Scientific and Technical Research Series; ISSN 1018-5593

Abstract
In this paper the laboratory test results on oxidation and release of ruthenium as a fission product element are summarised. The ruthenium appears in the nuclear fuel pellets of pressurized water reactors as one of the fission product elements during burnup. In case of severe accident when the air can contact the degraded hot fuel, the ruthenium oxidises and volatilizes.

The tests showed that during high-temperature oxidation of the Mo-Ru-Rh-Pd alloy in air flow the release rate of gaseous ruthenium oxides is reduced to 60-80% compared to the value measured in case of oxidation of pure metallic ruthenium powder in the same thermal-hydraulic conditions. Furthermore, if additional elements and chemical compounds representing other fission products were added in the alloy, a time delay of 30 to 60 minutes appeared in the release of gaseous ruthenium to the room-temperature environment similarly to earlier experiments conducted with the mixture of ruthenium powder and fission products.

One of the main results that in the outlet air flow reaching the environment the partial pressure of RuO_4 was far above what could be expected for room-temperature equilibrium conditions. It was pointed out that the highly volatile RuO_4 can decompose in solid, non-volatile RuO_2 and O_2. The X-ray fluorescence analysis results showed that some ruthenium compounds deposited on the colder circuit walls of the test facility. This suggests RuO_4 is not fully airstable, i.e., its stability in air can be limited in time.

The mission of the Joint Research Centre is to provide customer-driven scientific and technical support for the conception, development, implementation and monitoring of EU policies. As a service of the European Commission, the JRC functions as a reference centre of science and technology for the Union. Close to the policy-making process, it serves the common interest of the Member States, while being independent of special interests, whether private or national.